Surface roughness estimation of MBE grown CdTe/GaAs(211)B by ex-situ spectroscopic ellipsometry

Merve Karakaya,[1,a] Elif Bilgilisoy,[2] Ozan Arı,[2] and Yusuf Selamet[2]
[1]*Department of Material Science and Engineering, Izmir Institute of Technology, Izmir 35430, Turkey*
[2]*Department of Physics, Izmir Institute of Technology, Izmir 35430, Turkey*

(Received 13 March 2016; accepted 8 July 2016; published online 15 July 2016)

Spectroscopic ellipsometry (SE) ranging from 1.24 eV to 5.05 eV is used to obtain the film thickness and optical properties of high index (211) CdTe films. A three-layer optical model (oxide/CdTe/GaAs) was chosen for the ex-situ ellipsometric data analysis. Surface roughness cannot be determined by the optical model if oxide is included. We show that roughness can be accurately estimated, without any optical model, by utilizing the correlation between SE data (namely the imaginary part of the dielectric function, $<\varepsilon_2>$ or phase angle, ψ) and atomic force microscopy (AFM) roughness. $<\varepsilon_2>$ and ψ values at 3.31 eV, which corresponds to E_1 critical transition energy of CdTe band structure, are chosen for the correlation since E_1 gives higher resolution than the other critical transition energies. On the other hand, due to the anisotropic characteristic of (211) oriented CdTe surfaces, SE data ($<\varepsilon_2>$ and ψ) shows varieties for different azimuthal angle measurements. For this reason, in order to estimate the surface roughness by considering these correlations, it is shown that SE measurements need to be taken at the same surface azimuthal angle. Estimating surface roughness in this manner is an accurate way to eliminate cumbersome surface roughness measurement by AFM. [http://dx.doi.org/10.1063/1.4959223]

INTRODUCTION

Spectroscopic ellipsometry provides experimental data that can be modeled to obtain optical properties of the material. Ellipsometry allows one to obtain important aspects of the material such as alloy composition, surface temperature during growth, surface roughness etc.[1] In *in-situ* SE analysis, the surface roughness layer is in general modeled using effective medium approximation (EMA).[2,3] This model yields results that are in significant positive correlation with those obtained by AFM measurements.[4,5] However, in *ex-situ* SE data analysis, due to the formation of the oxide layer once the sample is exposed to air, EMA cannot give the correct surface roughness value if both EMA and oxide layer are used in the model. Therefore, only oxide layer can be used on the top layer of the optical model.[6]

CdTe is most widely used as a buffer layer between alternative substrates (such as GaAs, Si or Ge)[7–10] and HgCdTe, as an alternative to the standard substrate CdZnTe.[11,12] HgCdTe is the leading material for use in infrared detectors, especially for strategical applications.[13] The crystal quality and the surface roughness of the CdTe buffer layer are extremely important for the successful growth of HgCdTe by molecular beam epitaxy (MBE). Because of the large lattice mismatch between CdTe and the alternative substrates, some difficulties have been encountered in optimization of the growth process. Non-optimal growth conditions will negatively affect CdTe growth and, hence, HgCdTe

[a]E-mail; mervegunnar@iyte.edu.tr, Phone: +90 232 750 7686

epi-layer growth. Some undesired obstacles of the CdTe buffer layer, such as a large number of dislocations and other defects, and surface roughness, will deteriorate the crystal quality of HgCdTe; they hence need to be minimized by optimizing the growth conditions.

The (211) oriented surface is preferred for the MBE growth of HgCdTe focal plane array technology since this surface is free of common growth defects such as hillocks, oval defects, twinning, and antiphase domains that are present on other orientations such as (110), (100) and (111)B.[14] Te-terminated (211)B surface of CdTe is also required because this surface provides larger absorption of the Hg atoms to the surface.[15] HgCdTe IR detectors grown by MBE on CdTe/GaAs (211)B have being fabricated with good crystal quality and high operability.[8,16]

An atomically smooth surface of CdTe is required for the consecutive growth of HgCdTe. For this reason, characterization of surface properties is important. The most reliable surface roughness measurement method is AFM. However, this measurement may take a long time, and is also only carried out after growth on what is usually a limited sample size and limited local area. The measurement must be repeated at different positions to get an accurate measurement of overall surface roughness.

In this study, we show that surface roughness of CdTe/GaAs (211)B buffer layers can be determined by *ex-situ* SE data without constructing an optical model. Furthermore, the optical properties and thickness of the CdTe layers were determined exclusively by constructing an oxide/CdTe/GaAs optical model.

EXPERIMENTAL

The CdTe films were grown on epi-ready GaAs(211)B substrate by a Veeco Gen-20MZ MBE system. (211)B represents a B-phase (Te-terminated) CdTe (211) oriented surface. The samples mentioned in this paper were grown under various growth conditions and thicknesses between 0.3 and 6 μm. Protective oxides on GaAs surfaces were thermally removed under As_4 (or In) overpressure.[17–19] These de-oxidation processes were controlled by *in-situ* Reflection High Energy Electron Diffraction (RHEED), which yielded data related to surface crystal quality. Substrate temperature was controlled by pyrometer. After oxide removal, a CdTe nucleation layer was grown at a colder temperature (~210 °C) than that for CdTe film (~330 °C).[19] Before CdTe growth, the nucleation layer was annealed under Te_2 flux in order to stabilize the surface. The growth parameters are summarized in Table I.

TABLE I. Growth parameters of the samples.

	De-oxidation			Nucleation		Annealing		Growth	
Sample	Flux	Temp. (°C)	Time (min.)	Temp. (°C)	Time (min.)	Temp. (°C)	Time (min.)	Temp. (°C)	Time (min.)
1	As_4	561	12	250	5	-	-	370	60
2	As_4	580	5	320	5	-	-	350	80
3	As_4	577	4	261	5	-	-	331	90
4	As_4	585	5	280	1	-	-	310	90
5	As_4	586	4	280	0.5	-	-	300	120
6	As_4	650	4	252	0.5	-	-	310	110
7	As_4	600	16	250	0.5	-	-	310	263
8	As_4	580	4	220	10	390	5	305	120
9	As_4	583	4	220	10	380	5	295	120
10	As_4	582	4	218	10	388	5	295	120
11	As_4	582	4	218	10	388	5	295	120
12	As_4	525	15	208	10	385	4	295	70
13	In	488	2	206	10	382	5	298	120
14	In	532	3.5	203	10	387	4	295	70
15	In	526	3	210	10	383	4	305	70
16	In	529	3	204	10	384	4	305	180

Surface oxides of the substrates were thermally removed under As_4 flux for samples 1–11 and the de-oxidation temperatures were between 580 and 650 °C. The de-oxidation processes were carried out under In overpressure for samples 12-16, and oxide removal temperatures were between 488 and 532 °C according to pyrometer measurements. After oxide desorption of the substrate, a CdTe nucleation layer (~150 nm) was grown in order to achieve improved B-face nucleation and better crystallinity for the growth of the epitaxial CdTe layer. The nucleation processes were carried out at about 210 °C. After the growth of CdTe nucleation layer, an annealing was performed for samples at about 380 °C to improve the crystal quality and to prevent the formation of the treading dislocations for samples 8-16. Then, the CdTe layers were grown at about 300 °C. However, some samples (1-3) were grown at higher temperatures (330–370 °C).

A Woollam M-2000X ellipsometer was used to determine optical constant, thickness and surface roughness of the CdTe epilayers. Ellipsometric measurements were performed in ambient conditions. A Xenon arc lamp was used as a light source in measurements. The photon energy range was 1.24 eV to 5.05 eV. This range was divided into 479 numbers of wavelengths. The angle of incidence was constant at 65.82 ° for all measurements. Surface morphologies of epilayers were examined by AFM operated at semicontact mode.

DATA ANALYSIS

Ellipsometric data were fitted by constructing a three-layer optical model (oxide/CdTe/GaAs) to obtain the thicknesses and optical properties of CdTe films. The Woollam library of optical constants was used for GaAs substrate. For the top oxide layer the Couchy model, which is often used to obtain the dielectric function for transparent material, was used.[20] Nine general oscillators were used

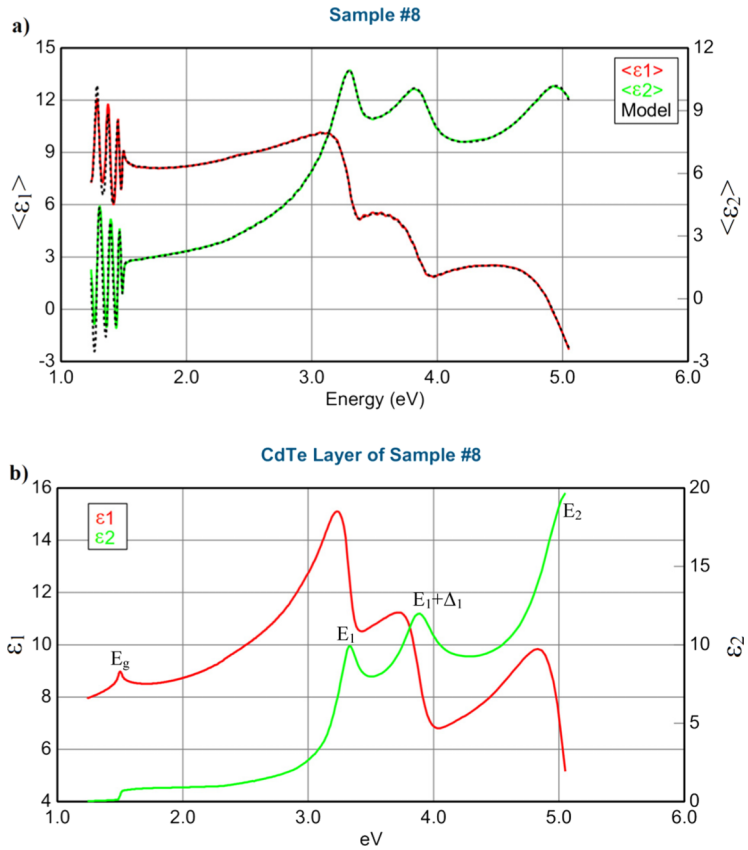

FIG. 1. (a) Experimental and model data of pseudo dielectric function and (b) CdTe dielectric function obtained by this fitting procedure for sample 8.

TABLE II. Thickness values and critical energies of CdTe obtained from ellipsometric data characterization and surface roughness values obtained from AFM.

	Thickness (nm)		Critical Energies of CdTe (eV)				
Sample	Oxide	CdTe	E_g	E_1	$E_1+\Delta_1$	E_2	AFM Surface Roughness (nm)
1	2.38	334.63	1.5144	3.3116	3.8522	5.0182	3.01
2	2.90	1174.39	1.5086	3.3115	3.8519	4.986	8.40
3	2.60	1361.28	1.5086	3.3117	3.8521	5.0182	13.76
4	2.30	1323.20	1.5085	3.3118	3.833	4.9858	7.03
5	2.77	1921.00	1.5086	3.3117	3.852	5.0182	10.63
6	3.47	1774.34	1.5143	3.3117	3.852	5.05	7.60
7	3.03	5054.17	1.5057	3.3258	3.871	–	22.08
8	4.63	2147.11	1.5028	3.3259	3.8901	–	14.36
9	3.06	2211.32	1.5143	3.3118	3.852	5.018	6.15
10	5.23	1978.23	1.5028	3.3257	3.8903	–	19.40
11	4.36	1956.25	1.5028	3.3257	3.8711	5.0182	8.66
12	4.32	2611.83	1.5028	3.3258	3.8904	–	19.00
13	3.38	3559.81	1.5114	3.3116	3.852	5.0181	4.10
14	3.78	2563.53	1.5114	3.3117	3.8518	5.0181	6.80
15	4.12	2551.38	1.5028	3.3258	3.8711	–	9.92
16	1.58	5817.88	1.5114	3.3117	3.8518	4.9859	4.96

to construct the dielectric function of CdTe epilayer, including Gaussian, Harmonic, Lorentzian and Pseni-Tri oscillators.[21,22] Here, thickness of oxide, thickness of CdTe and CdTe oscillator parameters (such as the amplitude at oscillator center energy, center energy, broadening etc.) were left free in the fit. Oxide thicknesses, CdTe film thicknesses and some critical transition energies of CdTe were obtained using this optical model for each sample. Sample 8 was chosen as a representative example and the measured pseudo dielectric function data and fitting results are given in Figure 1(a). As can be seen from the figure, the experimental data and the model were in close agreement for all samples, including this sample. The dielectric function of CdTe obtained from these fittings can be also seen in Figure 1(b) for sample 8. The peak of ε_1 at ~1.5 eV is related to photon absorption and band gap energy (E_g).[23]

The SE characterization results are summarized in Table II. The critical transition energies E_1, $E_1 + \Delta_1$, and E_2 were measured by using peaks of ε_2. E_1 energies were obtained as ~3.326 eV for samples 7, 8, 10, 11, 12 and 15; and E_1 ~3.312 eV for other samples. On the other hand, the samples that have E_1 ~3.326 eV also have E_g between 1.503 and 1.506 and $E_1 + \Delta_1$ between 3.871 and 3.890 eV. Other samples that have E_1 ~3.311 eV also have E_g between 1.508 and 1.514 eV and $E_1 + \Delta_1$ between 3.833 and 3.852 eV. These two groups are clearly distinguishable also in terms of ε_2 (Figure 2) and absorption coefficient (α) behavior (Figure 3). The samples were ranged according to their absorption coefficients at E_1, and absorption coefficients and E_1 critical energies for all samples were plotted in Figure 4 to show two distinct groups. These differences might be related to stress in the material due to thermal mismatch or incomplete relaxation of the CdTe epilayer.[24] Nevertheless, at room temperature, this effect is expected to be insignificant. The variation in ε_2 and α can be attributed to the relative density of imperfections in the crystallinity,[25] and the low absorption coefficient values can be associated with the void formation in the material.[26]

In our data analysis, oxide layer was used as the top layer due to best SE fit result. When we used EMA for the top layer, roughness values were neither physically meaningful nor consistent with AFM measurements. EMA layers with three components (CdTe, oxide and void) were also examined but unphysical surface roughness values were obtained. Therefore, the oxide/CdTe/GaAs model was chosen to analyze SE data for all samples. A new *ex-situ* data analysis was carried out to determine the surface roughness due to the insufficiency of this model in determining the surface roughness. In this new data analysis, peak intensities of the imaginary parts of the pseudo dielectric functions and psi functions at 3.31 eV were examined. A decrease of the ellipsometric data ($<\varepsilon_2>$ and ψ) intensity

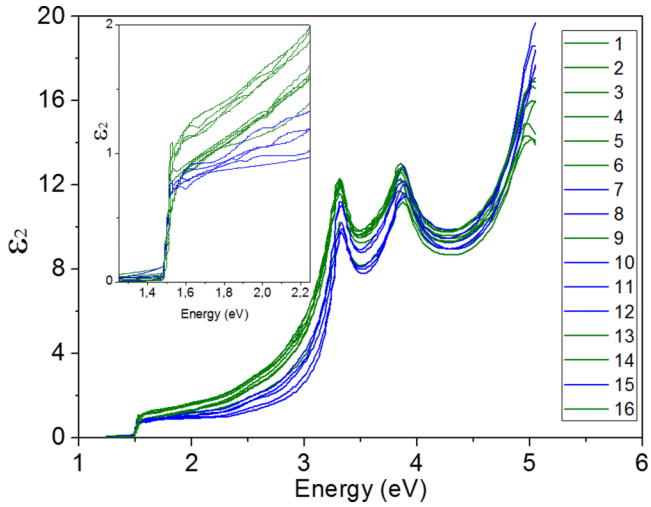

FIG. 2. The ε_2 functions for all samples. Green curves are ε_2 functions for samples 1, 2, 3, 4, 5, 6, 9, 13, 14 and 16, which have $E_1 \sim 3.31$ eV. Blue curves are for samples 7, 8, 10, 11, 12 and 15, which have $E_1 \sim 3.32$ eV.

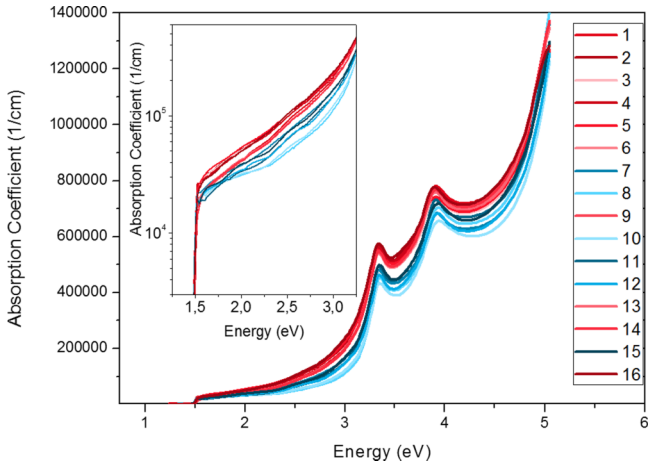

FIG. 3. The absorption coefficients for all samples. Red curves represent absorption coefficients of samples 1, 2, 3, 4, 5, 6, 9, 13, 14 and 16, which have $E_1 \sim 3.31$ eV. Blue curves represent absorption coefficients of samples 7, 8, 10, 11, 12 and 15, which have $E_1 \sim 3.32$ eV.

is consistently observed with increased surface roughness. The decrease was further analyzed by probing its correlation with AFM measurements.

RESULTS AND DISCUSSIONS

In SE data analysis, we used the pseudo dielectric function[27] as experimental data. The pseudo dielectric function is a function of energy dependent polarization angle (ψ and Δ) and angle of incidence (θ_i),

$$<\varepsilon> = \sin^2\theta_i \left[1 + \left(\frac{1 - \tan\psi e^{i\Delta}}{1 + \tan\psi e^{i\Delta}}\right)^2 \tan^2\theta_i\right]$$

Pseudo dielectric function is a complex quantity and it has real $<\varepsilon 1>$ and imaginary $<\varepsilon_2>$ parts,[28]

$$<\varepsilon> = <\varepsilon_1> + i\,<\varepsilon_2>$$

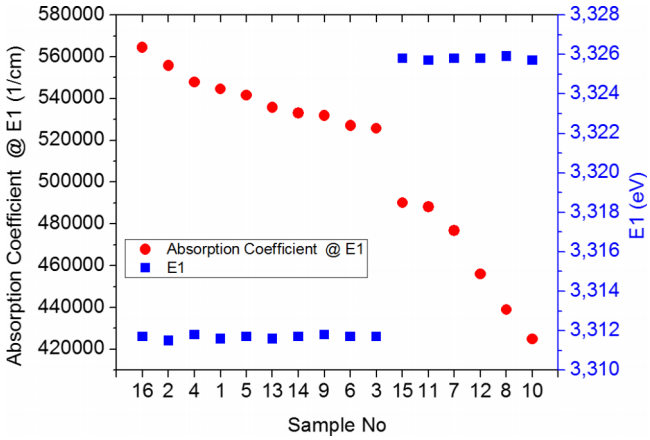

FIG. 4. Absorption coefficients at E_1 and E_1 critical energies for all samples. The samples were ranged according to their absorption coefficients, showing two distinct groups.

The surface morphology of a sample interferes with the correct determination of surface roughness because the ellipsometric measurements can display differences for the different azimuthal angles on the same point of the surface. These differences of the measured data vary according to the degree of surface anisotropy.[29] Anisotropy was found to be largest for the roughest surfaces. However, for the smoothest samples, slight anisotropy occurred. For this reason it is necessary to take ellipsometric data at the same azimuthal angle according to surface normal in order to determine the surface roughness from ellipsometric data analysis.

As the surface orientation of our samples was (211), therefore, other orientations (0-11) and (-111), which are perpendicular to the surface normal or parallel to the surface, were chosen as reference directions (Figure 6). The samples were mounted to the ellipsometer stage such that the (0-11) orientation of the sample was perpendicular to the incident light. The azimuthal angle was chosen as reference angle (0 °) for this position. The ellipsometric measurements were taken at 65.82 ° incident angle at room temperature. Imaginary parts of the pseudo dielectric functions of these samples, which were mounted on a sample stage such that incident light was perpendicular to the (0-11) orientation,

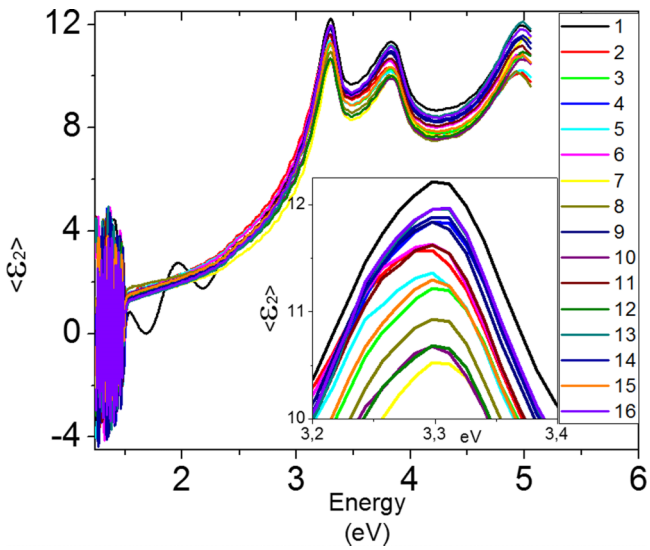

FIG. 5. Imaginary parts of pseudo dielectric functions of the samples. These functions were measured from the same directions, i.e. the incident light was perpendicular to the (0-11) orientation of the sample surface.

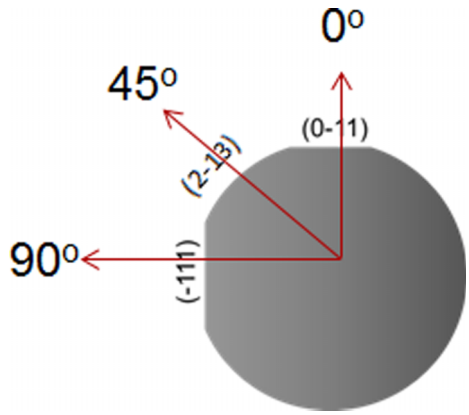

FIG. 6. Illustration of GaAs(211) wafer and its other orientations; (0-11) selected as 0° azimuthal angle, (2-13) corresponds to 45 ° azimuthal angle and (-111) corresponds to 90 ° azimuthal angle.

are given in Figure 5. A negative correlation was observed between surface roughness obtained by AFM and the imaginary part of the pseudo dielectric function (<ε_2>) intensity (Figure 7(a)). In order to further analyze this correlation we look at not only <ε_2> intensity but also ψ intensity at E_1 critical transition energy of CdTe band structure, which occurs around 3.31 eV. An exponential dependence

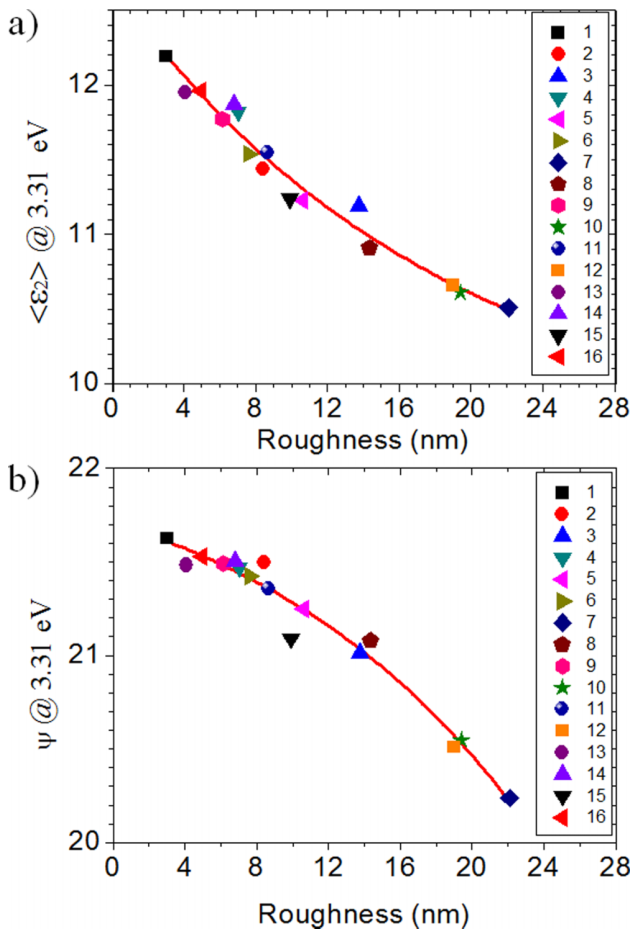

FIG. 7. (a) <ε_2> values at 3.31 eV and (b) ψ values at 3.31 eV versus surface roughness from AFM.

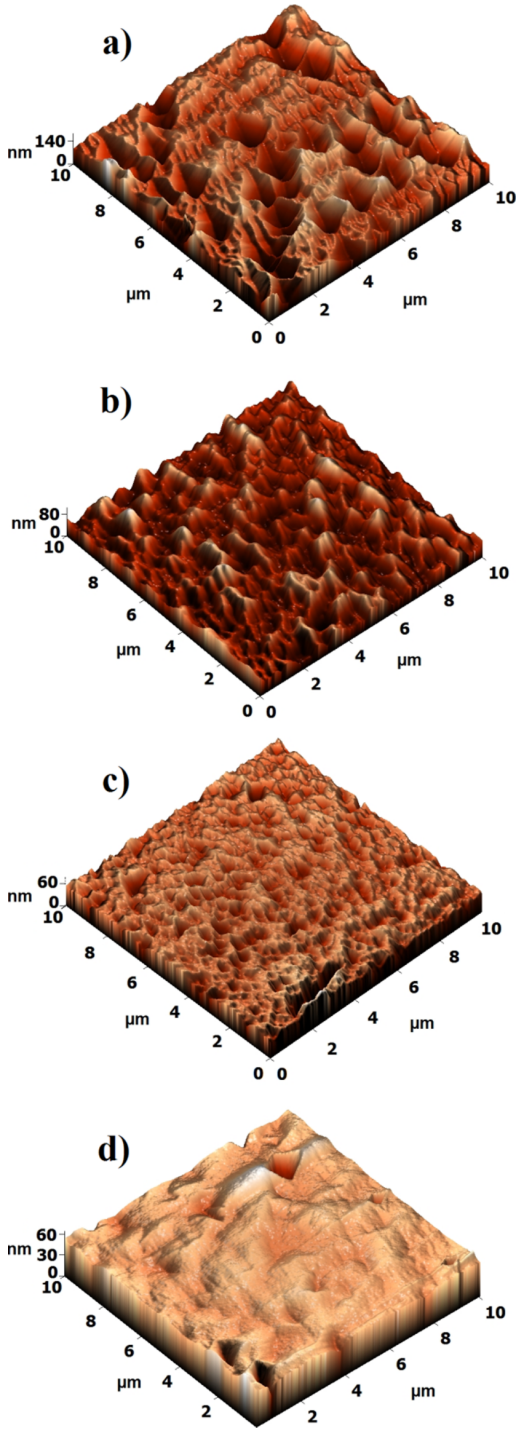

FIG. 8. AFM surface images of the (a) 7, (b) 8, (c) 9 and (d) 13. RMS values are 22.08 nm, 14.36 nm, 6.15 nm, 4.10 nm respectively.

(Figure 7) was obtained between these two intensities and surface roughness:

$$<\varepsilon_2> = 2.867\left[\exp\left(\frac{-d_{rough}}{15.951}\right)\right] + 9.793$$

$$\psi = -0.474\left[\exp\left(\frac{d_{rough}}{15.532}\right)\right] + 22.186$$

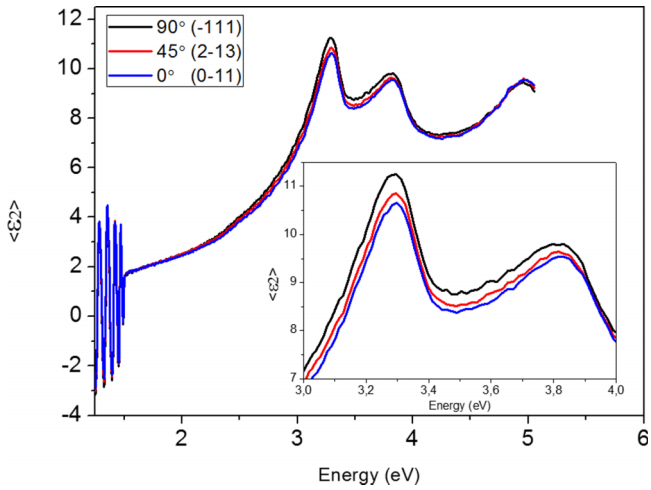

FIG. 9. Pseudo dielectric function data of sample 12 measured from three different orientations; Incident light was perpendicular to the (-111) orientation (black curve) and (0-11) orientation (blue curve) and (2-13) orientation (red curve). Due to the anisotropy, the intensity of the $<\varepsilon_2>$ values shows differences for this sample, having a surface roughness of 19 nm. The most explicit difference was shown at E1 transition point, 3.31 eV.

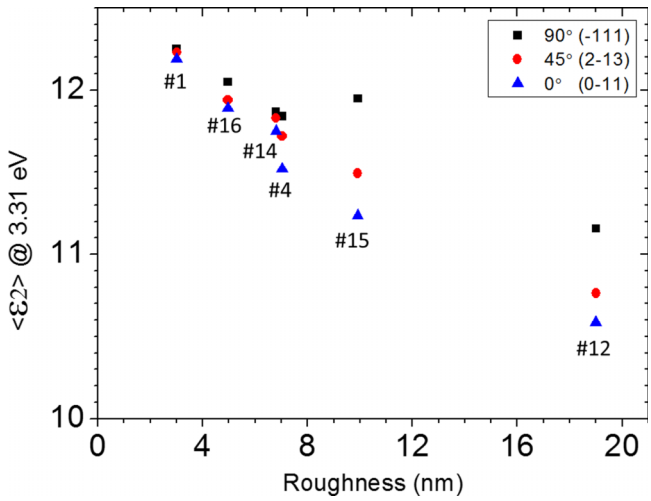

FIG. 10. For three different azimuthal angles, the peak values of $<\varepsilon_2>$ at 3.31 eV of the samples 1, 16, 14, 4, 15 and 12 versus the roughness values of these samples.

The adjustment R-square values were 0.973 and 0.965 for these two fittings $<\varepsilon_2>$ and ψ respectively. This relation was valid only for the 65.8 ° incident angle, room temperature and (211) oriented CdTe with zero degree azimuthal angle. The RMS roughness values were obtained from 10x10 μm^2 AFM scans. On the other hand, the spot size of the ellipsometer on the sample was about 2x7 mm^2 in size. Even though there is a large difference between the sizes of two measurement areas, correlation obtained was sufficiently acceptable. If it were possible to take the measurement on the same point of the sample from both AFM and SE, the correlation may be obtained with less error.

Fang et al. reported two different linear correlations between ψ and AFM roughness for two different chemically etched Si(100) samples,[30] examining ψ intensity at 1.96 eV (632.8 nm). This energy corresponds to HeNe laser operation energy used in their experiments, which is in the red part of the visible spectrum. On the other hand, E_1 critical transition energy of silicon is at 3.42 eV. We also examined ψ intensity at 1.96 eV for our samples and similarly obtained a linearly dependent correlation. However, some samples could not be fitted to this correlation. Therefore the E_1 transition

energy point 3.31 eV was considered appropriate for the determination of the CdTe surface roughness. It should be examined whether E_1 transition energy points of other semiconductor materials are appropriate for the determination of the surface roughness or not.

AFM surface images of samples 7, 8, 9 and 13 are given in Figure 8. RMS values were 22.08 nm, 14.36 nm, 6.15 nm, and 4.10 nm respectively. As it is known that there are three types of surfaces, mirror-like, hazy, and milky,[29] it can be said that sample 13 has a mirror-like surface and sample 7 has a hazy or milky surface. These hazy and milky surfaces have high anisotropy and we assume that these types of surfaces are more likely to occur on high indices orientations such as (211) due to non-optimal growth conditions.

Variation of intensity of $<\varepsilon_2>$ with azimuthal angle indicates an anisotropic surface.[31] Then, the anisotropy was checked by varying the azimuthal angle of the samples. Using sample 12 as an example, the pseudo dielectric function data measured from this sample at different azimuthal angles are given in Figure 9. When the incident light was perpendicular to the (0-11) or (2-13) or (-111) orientations, azimuthal angles were 0 °, 45 ° and 90 ° respectively. A variation of the intensity of the $<\varepsilon_2>$ values was observed with angle. As seen in Figure 9, the difference at E_1 transition point 3.31 eV is more pronounced compared to other transition points. In Figure 10, for three different azimuthal angles, the peak values of $<\varepsilon_2>$ at 3.31 eV of samples 1, 16, 14, 4, 15 and 12 versus the AFM roughness is also presented. A sort of proportionality between roughness and anisotropy can be observed, with higher roughness inducing larger anisotropy. We can infer from this that if we want to estimate the surface roughness using this method, it is necessary to always use the same azimuthal angle for measurement consistency. From data presented in this work, an incidence of 65.8 ° seems a sensible angle for the surface roughness estimation.

CONCLUSIONS

We used a three-layer optical model (oxide/CdTe/GaAs) to obtain the thickness and optical properties of CdTe films that were grown on GaAs(211) from *ex-situ* ellipsometric data analysis. However, surface roughness could not be obtained from the model with good agreement with AFM measurements obtained from other possible models, such as (roughness/oxide/CdTe/GaAs) or (roughness/CdTe/GaAs). In this study, we have shown that without constructing any optical model, roughness can be determined by using the exponentially dependent relations between SE data ($<\varepsilon_2>$ or ψ) and AFM roughness. It is also supposed that these relations will make determination of surface roughness easier during growth by *in-situ* ellipsometry. In the correlations, E_1 critical transition energy of CdTe band structure, which occurs around 3.31 eV, was chosen because it yielded better correlation between SE data and AFM roughness than the other critical transition energies. Due to the anisotropic surface characteristic of (211)B orientation, a certain azimuthal angle has to be chosen in consistent determination of surface roughness from SE data. This fast and reliable method would yield rapid feedback for the optimization of the growth process by minimizing surface roughness.

ACKNOWLEDGMENTS

This study was supported by the Gediz Project at Izmir Institute of Technology. The authors would like to thank all supporters for their assistance with the project.

[1] H. Fujiwara, *Spectroscopic ellipsometry: principles and applications* (John Wiley & Sons, 2007).
[2] D. Franta and I. Ohlídal, "Comparison of effective medium approximation and Rayleigh–Rice theory concerning ellipsometric characterization of rough surfaces," Optics communications **248**(4), 459-467 (2005).
[3] D. Aspnes, J. Theeten, and F. Hottier, "Investigation of effective-medium models of microscopic surface roughness by spectroscopic ellipsometry," Physical Review B **20**(8), 3292 (1979).
[4] H. Fujiwara *et al.*, "Assessment of effective-medium theories in the analysis of nucleation and microscopic surface roughness evolution for semiconductor thin films," Physical Review B **61**(16), 10832 (2000).
[5] J. Li *et al.*, "Spectroscopic ellipsometry studies of thin film CdTe and CdS: From dielectric functions to solar cell structures," *Photovoltaic Specialists Conference (PVSC), 2009 34th IEEE* (IEEE, 2009).
[6] F. Peiris *et al.*, "Exploring the Optical Properties of Hg1- x Cd x Se Films Using IR-Spectroscopic Ellipsometry," Journal of Electronic Materials **43**(8), 3056-3059 (2014).

[7] J. Zanatta *et al.*, "Molecular beam epitaxy growth of HgCdTe on Ge for third-generation infrared detectors," Journal of electronic materials **35**(6), 1231-1236 (2006).
[8] J. Arias *et al.*, "Infrared diodes fabricated with HgCdTe grown by molecular beam epitaxy on GaAs substrates," Applied Physics Letters **54**(11), 1025-1027 (1989).
[9] T. De Lyon *et al.*, "Heteroepitaxy of HgCdTe (112) infrared detector structures on Si (112) substrates by molecular-beam epitaxy," Journal of Electronic Materials **25**(8), 1341-1346 (1996).
[10] L. He *et al.*, "MBE HgCdTe on Si and GaAs substrates," Journal of Crystal Growth **301**, 268-272 (2007).
[11] M. Daraselia *et al.*, "In-situ control of temperature and alloy composition of Cd1–xZnxTe grown by molecular beam epitaxy," Journal of Electronic Materials **29**(6), 742-747 (2000).
[12] Y. Chang *et al.*, "Near-bandgap infrared absorption properties of HgCdTe," Journal of electronic materials **33**(6), 709-713 (2004).
[13] W.E. Tennant *et al.*, "Key issues in HgCdTe-based focal plane arrays: An industry perspective," Journal of Vacuum Science & Technology B **10**(4), 1359-1369 (1992).
[14] J. Arias *et al.*, "Molecular-beam epitaxy growth and insitu arsenic doping of p-on-n HgCdTe heterojunctions," Journal of applied physics **69**(4), 2143-2148 (1991).
[15] G. Badano *et al.*, "In-situ ellipsometry studies of adsorption of Hg on CdTe (211) B/Si (211) and molecular beam epitaxy growth of HgCdTe (211) B," Journal of electronic materials **33**(6), 583-589 (2004).
[16] J. Wenisch *et al.*, "Evaluation of HgCdTe on GaAs Grown by Molecular Beam Epitaxy for High-Operating-Temperature Infrared Detector Applications," Journal of Electronic Materials 1-5 (2015).
[17] L. Li *et al.*, "In-assisted desorption of native GaAs surface oxides," Applied Physics Letters **99**(6), 061910 (2011).
[18] R. Jacobs *et al.*, "Development of MBE II–VI Epilayers on GaAs (211) B," Journal of electronic materials **41**(10), 2707-2713 (2012).
[19] O. Arı *et al.*, "MBE-Grown CdTe Layers on GaAs with In-assisted Thermal Deoxidation," Journal of Electronic Materials 1-6.
[20] M. Rebien *et al.*, "Optical properties of gallium oxide thin films," Applied physics letters **81**(2), 250-252 (2002).
[21] J. Khoshman *et al.*, "Multiple oscillator models for the optical constants of polycrystalline zinc oxide thin films over a wide wavelength range," Applied Surface Science **307**, 558-565 (2014).
[22] C.M. Herzinger and B.D. Johs, *Dielectric function parametric model, and method of use* (Google Patents, 1998).
[23] C.C. Kim and S. Sivananthan, "Modeling the optical dielectric function of II-VI compound CdTe," Journal of applied physics **78**(6), 4003-4010 (1995).
[24] P. Etchegoin *et al.*, "Piezo-optical response of Ge in the visible–uv range," Physical Review B **45**(20), 11721 (1992).
[25] A. Ramirez *et al.*, "Giant dielectric constant response in a copper-titanate," Solid State Communications **115**(5), 217-220 (2000).
[26] S. Minoura *et al.*, "Dielectric function of Cu (In, Ga) Se2-based polycrystalline materials," Journal of Applied Physics **113**(6), 063505 (2013).
[27] S. L. Ren *et al.*, "Dielectric function of solid C70 films," Applied physics letters **61**(2), 124-126 (1992).
[28] D. Aspnes and A. Studna, "Dielectric functions and optical parameters of si, ge, gap, gaas, gasb, inp, inas, and insb from 1.5 to 6.0 ev," Physical Review B **27**(2), 985 (1983).
[29] G. Badano *et al.*, "Anisotropic Surface Roughness in Molecular-Beam Epitaxy CdTe (211) B/Ge (211)," Journal of Electronic Materials **37**(9), 1369-1375 (2008).
[30] S. Fang *et al.*, "Comparison of Si surface roughness measured by atomic force microscopy and ellipsometry," Applied physics letters **68**(20), 2837-2839 (1996).
[31] G. Badano, X. Baudry, and I.C. Robin, "In Situ Spectroscopic Ellipsometry of Rough Surfaces: Application to CdTe (211) B/Ge (211) Grown by Molecular-Beam Epitaxy," Journal of electronic materials **38**(8), 1652-1660 (2009).